Mon. Not. R. Astron. Soc. **363,** 469–478 (2005) doi:10.1111/j.1365-2966.2005.09393.x

Probing decisive answers to dark energy questions from cosmic complementarity and lensing tomography

Mustapha Ishak[1,2]★

[1]*Department of Astrophysical Sciences, Princeton University, Princeton, NJ 08544, USA*
[2]*Department of Physics, The University of Texas at Dallas, Richardson, TX 75083, USA*

Accepted 2005 July 1. Received 2005 June 23; in original form 2005 March 1

ABSTRACT

We study future constraints on dark energy parameters determined from several combinations of cosmic microwave background experiments, supernova data, and cosmic-shear surveys with and without tomography. In this analysis, we look in particular for combinations of experiments that will bring the uncertainties to a level of precision tight enough (a few per cent) to answer decisively some of the questions regarding dark energy. In view of the parametrization dependence problems, we probe the dark energy using two variants of its equation of state $w(z)$, and its energy density $\rho_{\rm de}(z)$. For the latter, we model $\rho_{\rm de}(z)$ as a continuous function interpolated using dimensionless parameters $\mathcal{E}_i(z_i) \equiv \rho_{\rm de}(z_i)/\rho_{\rm de}(0)$. We consider a large set of 13 cosmological and systematic parameters, and assume reasonable priors on the lensing and supernova systematics. For the CMB, we consider future constraints from eight years of data from *WMAP*, one year of data from *Planck*, and one year of data from the Atacama Cosmology Telescope (ACT). We use two sets of 2000 supernovae with $z_{\rm max} = 0.8$ and 1.5 respectively, and consider various cosmic-shear reference surveys: a wide ground-based-like survey, covering 70 per cent of the sky, and with successively two and five tomographic bins; and a deep-space-based-like survey with 10 tomographic bins and various sky coverages. The 1σ constraints found are $\{\sigma(w_0) = 0.086, \sigma(w_1) = 0.069\}$, $\{\sigma(w_0) = 0.088, \sigma(w_a) = 0.11\}$, and $\{\sigma(\mathcal{E}_1) = 0.029, \sigma(\mathcal{E}_2) = 0.065\}$ from *Planck*, supernovae and the ground-based-like lensing survey with two bins. When five bins are used within the same combination the constraints reduce to $\{\sigma(w_0) = 0.04, \sigma(w_1) = 0.034\}$, $\{\sigma(w_0) = 0.041, \sigma(w_a) = 0.056\}$, and $\{\sigma(\mathcal{E}_1) = 0.012, \sigma(\mathcal{E}_2) = 0.049\}$. Finally, when the deep lensing survey with 10 per cent coverage of the sky and 10 tomographic bins is used along with *Planck* and the deep supernova survey, the constraints reduce to $\{\sigma(w_0) = 0.032, \sigma(w_1) = 0.027\}$, $\{\sigma(w_0) = 0.033, \sigma(w_a) = 0.04\}$, and $\{\sigma(\mathcal{E}_1) = 0.01, \sigma(\mathcal{E}_2) = 0.04\}$. Other coverages of the sky and other combinations of experiments are explored as well. Although some worries remain about other systematics, our study shows that, after the combination of the three probes, lensing tomography with many redshift bins and large coverages of the sky has the potential to add key improvements to the dark energy parameter constraints. However, the fact that very ambitious and sophisticated surveys are required in order to achieve some of these constraints or to improve them suggests the need for new tests to probe the nature of dark energy in addition to constraining its equation of state.

Key words: gravitational lensing – cosmology: theory – dark matter – large-scale structure of Universe.

1 INTRODUCTION

One of the most important and challenging problems in cosmology and particle physics is to understand the nature of the dark energy that is driving the observed cosmic acceleration (see, for example, Weinberg 1989; Carroll et al. 1992; Turner 2000; Sahni & Starobinsky 2000; Padmanabhan 2003; Ishak 2005). An important approach to this problem is to constrain the properties of dark energy using cosmological probes. This should provide measurements that allow the various competing models of dark energy to be tested. As a result of the high degeneracy within a particular narrow range of

★E-mail: mishak@princeton.edu

the parameter space, however, it will be difficult to constrain conclusively dynamical dark energy models, and much effort and strategic planning will be needed. Ultimately, a combination of powerful cosmological probes and tests will be necessary.

In this paper, we study how dark energy parameters are constrained from different combinations of cosmic microwave background (CMB) experiments, data from Type Ia supernovae (SNe Ia), and weak lensing (WL) surveys with and without tomography. In particular, we look for combinations of experiments that can constrain these parameters well enough to settle decisively, say to a few per cent, some of the dark energy questions. When CMB measurements constrained the total energy density to $\Omega_{\rm T} = 1.02 \pm 0.02$ to the 1σ level (Spergel et al. 2003; Bennet et al. 2003), it became generally more accepted that spatial curvature is negligible. Thus, an uncertainty of a few per cent on dark energy parameters could be set as a reasonable goal. Of course, one should bear in mind that it will always remain possible to construct dynamical dark energy models that are indistinguishable from a cosmological constant model within these limits, and therefore it is necessary to resort to cosmological tests beyond the equation of state measurements. A better scenario for providing a decisive answer would be one in which it could be clearly shown that dark energy is not a cosmological constant.

It is certainly wise to probe the nature of dark energy using gradual steps. However, in both of the scenarios mentioned above, it should be kept in mind that the results and conclusions obtained from an analysis in which the equation of state is assumed constant are subject to changes if the equation of state is allowed to vary with the redshift. In this paper, we consider dark energy with a varying equation of state.

We chose the combination CMB+SN Ia+WL, as various studies have already shown that Type Ia supernovae constitute a powerful probe of dark energy via distance–redshift measurements (see, for example, Riess et al. 1998; Garnavich et al. 1998; Filippenko & Riess 1998; Perlmutter et al. 1997, 1999; Riess et al. 2000, 2001; Tonry et al. 2003; Knop et al. 2003; Barris et al. 2004; Riess et al. 2004). Furthermore, several parameter forecast studies have shown that combining constraints from weak gravitational lensing with constraints from the CMB is a powerful way to constrain dark energy (see, for example, Hu 2001; Huterer 2002; Huterer & Turner 2001; Benabed & Van Waerbeke 2004; Abazajian & Dodelson 2003; Refregier et al. 2003; Heavens 2003; Simon, King & Schneider 2004; Jain & Taylor 2003; Bernstein & Jain 2004; Song & Knox 2005). Importantly, weak lensing measurements are sensitive both to the effect of dark energy on the expansion history and to its effect on the growth factor of large-scale structure. Furthermore, in addition to tightening the constraints, the use of independent probes will allow the systematic errors of each probe to be tested, these being serious limiting factors in these studies. For each of these probes, many data will be available in the near and distant future. For WL, there are many ongoing, planned and proposed surveys, such as the Deep Lens Survey (http://dls.bell-labs.com/) (Wittman 2002); the NOAO Deep Survey (http://www.noao.edu/noao/noaodeep/); the Canada-France-Hawaii Telescope (CFHT) Legacy Survey (http://www.cfht.hawaii.edu/Science/CFHLS/) (Mellier et al. 2001); the Panoramic Survey Telescope and Rapid Response System (http://pan-starrs.ifa.hawaii.edu/); the Supernova Acceleration Probe (SNAP; http://snap.lbl.gov/) (Rhodes et al. 2004; Massey et al. 2004; Refregier et al. 2004); and the Large Synoptic Survey Telescope (LSST; http://www.lsst.org/lsst_home.html) (Tyson 2002). Similarly, there are many ongoing, planned and proposed SNe Ia surveys, such as the Supernova Legacy Survey (SNLS) (Pain et al. 2002; Pritchet 2005); The Nearby Supernova Factory (SNfactory) (Wood-Vasey et al. 2004); the ESSENCE project (Smith et al. 2002; Garnavich et al 2002; Kirshner et al. 2003); the Sloan Digital Sky Survey (SDSS) (Madgwick et al. 2003); The Carnegie Supernova Project (Freedman 2004); and the Dark Energy Camera Project (http://home.fnal.gov/annis/astrophys/deCam/). It should be noted that there are other cosmological tools for probing dark energy that have not been considered in this study, notably clusters of galaxies (see, for example, Mohr 2005; Wang 2003, and references therein), Lyman-α forests (see, for example, Mandelbaum et al. 2003; Seljak et al. 2005), and baryonic oscillations (see, for example, Eisenstein 2002; Seo & Eisenstein 2003; Blake & Glazebrook 2003; Linder 2003b).

For the CMB, we consider future constraints from 8 yr of data from the Wilkinson Microwave Anisotropy Probe (*WMAP*8) (Bennet et al. 2003; Spergel et al. 2003), 1 yr of data from the *Planck* satellite (PLANCK1), and 1 yr of data from the Atacama Cosmology Telescope (ACT) (see, for example, Kosowsky et al. 2003). We use two sets of 2000 supernovae with $z_{\rm max} = 0.8$ and $z_{\rm max} = 1.5$ respectively, and consider two types of cosmic-shear surveys: a ground-based-like survey covering 70 per cent of the sky with the source-galaxy redshift distribution having a median redshift of $z_{\rm med} \approx 1$, and a space-based-like deep survey covering successively 1, 10 and 70 per cent of the sky, with $z_{\rm med} \approx 1.5$.

We take into account systematic limits for the supernovae by adding a systematic uncertainty floor in quadrature following Kim et al. (2004). We also include, for weak lensing, the effect of the redshift bias and the shear calibration bias by adding and marginalizing over the corresponding parameters as in Ishak et al. (2004).

The constraints on the dark energy equation of state are parametrization-dependent (see, for example, Wang & Tegmark 2004; Upadhye, Ishak & Steinhardt 2005). Moreover, there is a smearing effect owing to the double integration involved when using the equation of state (Maor et al. 2001, 2002). In order partially to avoid this, one could probe the variations in the dark energy density directly using the data (see, for example, Wang & Mukherjee 2004; Wang & Freese 2004). However, it has been argued that the equation of state is more physically realistic, as it also contains information on the pressure, and trying to probe the equation of state from the density leads to instability and bias (Linder 2004). Therefore, we choose in this analysis to use both and to parametrize the dark energy using its density $\rho_{\rm de}(z)$ as well as two different parametrizations of its equation of state $w(z)$.

2 COSMOLOGICAL MODEL AND DARK ENERGY PARAMETRIZATION

2.1 The model

A set of 13 parameters is considered as follows. For constraints from WL, we use $\Omega_{\rm m}h^2$, the physical matter density; Ω_Λ, w_0 and w_1 (or w_a), respectively the fraction of the critical density in a dark energy component and its equation of state parameters (see Section 2.2) (alternatively, we use the dark energy density parameters $\mathcal{E}_i \equiv \rho_{\rm de}(z_i)/\rho_{\rm de}(0)$ with $i = 1, 2$: see Section 2.2); we use $n_{\rm s}$ ($k_0 = 0.05\,h\,{\rm Mpc}^{-1}$) and $\alpha_{\rm s}$, the spectral index and running of the primordial scalar power spectrum at k_0; and $\sigma_8^{\rm lin}$, the amplitude of linear fluctuations. In order to parametrize some systematics, we include as a parameter $z_{\rm p}$, the characteristic redshift of source galaxies (see equation 13), as well as $\zeta_{\rm s}$ and $\zeta_{\rm r}$, the calibration parameters defined in Ishak et al. (2004) that determine the absolute calibration error on the lensing power spectrum (Hirata & Seljak 2003), and the

relative calibration between tomography bins (see Section 3.4). When we combine this set of parameters with the CMB, we include $\Omega_b\ h^2$, the physical baryon density; τ, the optical depth to reionization; and T/S the scalar–tensor fluctuation ratio. We assume a spatially flat universe with $\Omega_m + \Omega_\Lambda = 1$. This fixes Ω_m and H_0 as functions of the basic parameters. We do not include massive neutrinos, or primordial isocurvature perturbations. For the supernova analysis, we use Ω_Λ, w_0, w_1 (or $\mathcal{E}_1$, $\mathcal{E}_2$), and treat the magnitude parameter $\mathcal{M}$ as a nuisance parameter. We use the fiducial model (e.g. Spergel et al. 2003) and add w_0 and w_1: $\Omega_b\ h^2 = 0.0224$, $\Omega_m\ h^2 = 0.135$, $\Omega_\Lambda = 0.73$, $w_0 = -1.0$, $w_1 = 0.0$, $n_s = 0.93$, $\alpha_s = -0.031$, $\sigma_8 = 0.84$, $\tau = 0.17$, $T/S = 0.2$, $z_p = 0.76, 1.12$, $\zeta_s = 0.0$, and $\zeta_r = 0.0$.

2.2 Dark energy parametrization

As mentioned earlier, constraining the dark energy using its equation of state is known to be parametrization-dependent (see, for example, Wang & Tegmark 2004; Upadhye et al. 2005), and also to suffer from a smearing owing to the double integration involved (Maor et al. 2001, 2002). Alternatively, it is possible to probe the variations of the dark energy density directly as a function of redshift $\rho_{de}(z)$. It has, however, been pointed out that the equation of state contains information on both the density and pressure of the dark energy, and that using the density to probe the equation of state may lead to instability and bias (Linder 2004). We chose to study the constraints on dark energy using both approaches.

2.2.1 The equation of state

There are several parametrizations of the dark energy equation of state that have been used to study currently available data or to perform parameter constraint projections. Discussions of the advantages and drawbacks of some of these parametrizations can be found in Wang & Tegmark (2004) and Upadhye et al. (2005). The following two parametrizations, which have no divergence at very large redshift, are used here.

(i) $(w_0,\ w_1)$ (1)

Here w_1 represents the redshift derivative of $w(z)$ in the recent past as follows (see, for example, Upadhye et al. 2005):

$$w(z) = \begin{cases} w_0 + w_1 z & \text{if } z < 1 \\ w_0 + w_1 & \text{if } z \geqslant 1. \end{cases} \quad (2)$$

The evolution of dark energy density with redshift is given by $\rho_{de}(z) = \rho_{de}(0)\mathcal{E}(z)$, where

$$\mathcal{E}(z) \equiv \begin{cases} (1+z)^{3(1+w_0-w_1)}\ \mathrm{e}^{3w_1 z} & \text{if } z < 1, \\ (1+z)^{3(1+w_0+w_1)}\ \mathrm{e}^{3w_1(1-2\ln 2)} & \text{if } z \geqslant 1. \end{cases} \quad (3)$$

(ii) $(w_0,\ w_a)$ (4)

Here the equation of state is parametrized as (Chevalier et al. 2001; Linder 2003a)

$$w(a) = w_0 + w_a \frac{z}{1+z} = w_0 + w_a(1-a), \quad (5)$$

where a is the scale factor. The dark energy density evolves with $\mathcal{E}(a)$, now given by

$$\mathcal{E}(a) = a^{-3(1+w_0+w_a)}\mathrm{e}^{-3w_a(1-a)}. \quad (6)$$

2.2.2 The density parameters: $\mathcal{E}_1 \equiv \rho_{de}(z_1)/\rho_{de}(0)$, $\mathcal{E}_2 \equiv \rho_{de}(z_2)/\rho_{de}(0)$

Following Wang & Mukherjee (2004) and Wang & Freese (2004), we parametrize $\mathcal{E}(z) \equiv \rho_{de}(z)/\rho_{de}(0)$ as a continuous function interpolated between today and its amplitude parameters $\mathcal{E}_1$ and $\mathcal{E}_2$, corresponding respectively to $z = 0.5$ and 1.0, and remaining constant at higher redshifts. We use a polynomial interpolation as in (Wang & Mukherjee 2004; Wang & Freese 2004), so

$$\mathcal{E}(z) = 1 + (4\mathcal{E}_1 - \mathcal{E}_2 - 3)\frac{z}{z_{max}} + 2(\mathcal{E}_2 - 2\mathcal{E}_1 + 1)\frac{z^2}{z_{max}^2}, \quad (7)$$

where the parameters $\mathcal{E}_1$ and $\mathcal{E}_2$ will be constrained from the data. As suggested in (Wang & Mukherjee 2004) and (Wang & Freese 2004), we could use more than two density parameters as many more data will be available in the future, but we chose to use only two parameters in order to keep the number of parameters equal to in the equation of state case and be able to make a fair comparison of the results. Departures of the density parameters from unity will be an indication of a redshift evolution of the dark energy density and will rule out a cosmological constant.

3 PROBING DARK ENERGY WITH COSMIC SHEAR

Weak lensing is a very promising tool for an era of precision cosmology. Several studies have already used currently available cosmic-shear data to constrain various cosmological parameters (Contaldi et al. 2003; Van Waerbeke et al. 2002; Wang et al. 2003; Jarvis et al. 2003; Massey et al. 2005). By using statistical inference theory, many other studies have demonstrated the potential of this probe (Hu & Tegmark 1999; Hu 2001; Huterer 2002; Abazajian & Dodelson 2003; Benabed & Van Waerbeke 2004; Takada & Jain 2004; Takada & White 2004; Heavens 2003; Jain & Taylor 2003; Bernstein & Jain 2004; Ishak et al. 2004; Simon et al. 2004). In particular, weak lensing has been shown to constrain significantly the dark energy parameters. The advantage of weak lensing is that it is sensitive to the effect of dark energy on the expansion history and to its effect on the growth factor of large-scale structure. A further advantage of weak lensing is that it allows the construction of new tests or techniques to probe cosmology. These include redshift-bin tomography (Hu 1999, 2002), cross-correlation cosmography (Bernstein & Jain 2004), and the use of higher-order statistics such as the bispectrum (see, for example, Takada & Jain 2004). We explore in this analysis the constraints obtained from the convergence power spectrum and multiple-bin tomography.

3.1 Convergence power spectrum

Light rays travelling to us from background galaxies are deflected by mass fluctuations in large-scale structures. This results in distortions of the sizes and shapes of these galaxies that can be described by the transformation matrix

$$A_{ij} \equiv \frac{\partial \theta_s^i}{\partial \theta^j} = \begin{pmatrix} 1-\kappa-\gamma_1 & \gamma_2 \\ \gamma_2 & 1-\kappa+\gamma_1 \end{pmatrix}, \quad (8)$$

where $\boldsymbol{\theta}_s$ is the angular position in the source plane; $\boldsymbol{\theta}$ is the angular position in the image plane; κ is the convergence and describes the magnification of the size of the image; and γ_1 and γ_2 are the components of the complex shear and describe the distortion of the shape of the image. In the weak gravitational lensing limit, $|\kappa|$ and $|\gamma| \ll 1$.

The convergence is given by a weighted projection of the matter–energy density fluctuations $\delta \equiv \delta\rho/\rho$ along the line of sight between the source and the observer:

$$\kappa(\hat{\theta}) = \int_0^{\chi_{\rm H}} W(\chi)\delta(\chi, \chi\hat{\theta})\,{\rm d}\chi, \tag{9}$$

where χ is the radial comoving coordinate and $\chi_{\rm H}$ is the comoving coordinate at the horizon.

The convergence scalar field can be decomposed into multipole moments of the spherical harmonics as

$$\kappa(\hat{\theta}) = \sum_{lm} \kappa_{lm} Y_l^m(\hat{\theta}), \tag{10}$$

where

$$\kappa_{lm} = \int {\rm d}\hat{\theta}\kappa(\hat{\theta}, \chi) Y_l^{m*}(\hat{\theta}). \tag{11}$$

The convergence power spectrum P_l^κ is then defined by

$$\langle \kappa_{lm}\kappa_{l'm'}\rangle = \delta_{ll'}\delta_{mm'}P_l^\kappa, \tag{12}$$

and we will use it as our weak lensing statistic. In the Limber approximation, it is given by (Kaiser 1992; Jain & Seljak 1997; Kaiser 1998)

$$P_l^\kappa = \frac{9}{4}H_0^4\Omega_{\rm m}^2 \int_0^{\chi_{\rm H}} \frac{g^2(\chi)}{a^2(\chi)} P_{\rm 3D}\left[\frac{l}{\sin_K(\chi)}, \chi\right] {\rm d}\chi, \tag{13}$$

where $P_{\rm 3D}$ is the 3D non-linear power spectrum of the matter density fluctuation, δ; $a(\chi)$ is the scale factor; and $\sin_K\chi = K^{-1/2}\sin(K^{1/2}\chi)$ is the comoving angular diameter distance to χ. (For the spatially flat universe used in this analysis, this reduces to χ.) The weighting function $g(\chi)$ is the source-averaged distance ratio given by

$$g(\chi) = \int_\chi^{\chi_{\rm H}} n(\chi')\frac{\sin_K(\chi'-\chi)}{\sin_K(\chi')}\,{\rm d}\chi', \tag{14}$$

where $n(\chi(z))$ is the source redshift distribution normalized by $\int {\rm d}z\, n(z) = 1$. For $n(z)$, we use the distribution

$$n(z) = \frac{z^2}{2z_0^3}\,{\rm e}^{-z/z_0} \tag{15}$$

(Wittman et al. 2000), which peaks at $z_{\rm p} = 2z_0$. For cosmic-shear calculations, we integrate the growth factor numerically using

$$G'' + \left[\frac{7}{2} - \frac{3}{2}\frac{w(a)}{1+X(a)}\right]\frac{G'}{a} + \frac{3}{2}\frac{1-w(a)}{1+X(a)}\frac{G}{a^2} = 0 \tag{16}$$

(Linder & Jenkins 2003), where $G = D/a$ is the normalized growth factor with $D = \delta(a)/\delta(a_i)$;

$$X(a) = \frac{\Omega_{\rm m}}{(1-\Omega_{\rm m})a^3\mathcal{E}(a)}; \tag{17}$$

and $\mathcal{E}(a)$ is as given in equation (4). We use the mapping procedure HALOFIT (Smith et al. 2003) to calculate the non-linear power spectrum. We show in Fig. 1 the convergence power spectra for the 10 tomographic bins. We also show the sample variance errors averaged over bands in l.

3.2 Weak lensing tomography

The separation of source galaxies into tomographic bins significantly improves the constraints on cosmological parameters, and particularly those of dark energy because tomography probes the growth of structure. The constraints obtained within the various redshift bins are complementary and combine to reduce the final uncertainties. We explore here three tomography studies using two different types of cosmic-shear surveys. For the first survey (ground-based-like), the source-galaxy redshift distribution has a median redshift $z_{\rm median} = 1.0$, and we assume that knowledge of the photometric redshift will allow the source galaxies to be split into successively two and five bins. For the second survey (space-based-like), the source-galaxy redshift distribution has a median redshift $z_{\rm median} = 1.5$, and we assume a good knowledge of photometric redshifts and split the sources into 10 tomographic bins. For each redshift bin i, the weighting function is given by

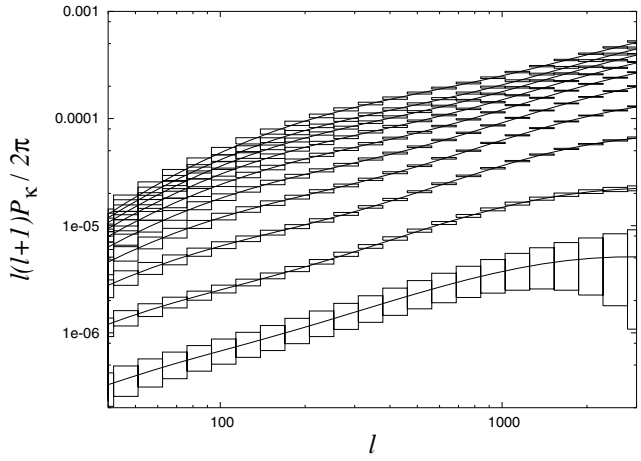

Figure 1. Convergence auto power spectra for the 10 tomography bins. All the parameters are fixed at their fiducial values. From the bottom to the top, the curves correspond to the redshift intervals [0.0,0.3], . . . ,[2.7,3.0]. For each curve, the sample variance errors are displayed averaged over bands in l.

$$g_i(\chi) = \begin{cases} \displaystyle\int_{\chi_i}^{\chi_{i+1}} {\rm d}\chi' n_i(\chi')\frac{\chi'-\chi}{\chi'}, & \chi \leqslant \chi_{i+1} \\ 0, & \chi > \chi_{i+1} \end{cases}, \tag{18}$$

where $n_i(\chi)$ is the bin-normalized redshift distribution. The average number density of galaxies in this bin is $\Phi_i\bar{n}$, with the fraction Φ_i given by

$$\Phi_i = \int_{\chi_i}^{\chi_{i+1}} {\rm d}\chi' n(\chi'). \tag{19}$$

For example, in the two-bin case, the normalized distributions are given by

$$n^{\rm A}(z) = \begin{cases} \dfrac{n(z)}{1-5/e^2} & z_{\rm p} \leqslant 2z_0, \\ 0, & z_{\rm p} > 2z_0, \end{cases} \tag{20}$$

and

$$n^{\rm B}(z) = \begin{cases} 0, & z_{\rm p} \leqslant 2z_0, \\ \dfrac{n(z)}{5/e^2} & z_{\rm p} > 2z_0. \end{cases} \tag{21}$$

For the five bins, we use redshift intervals of $\Delta z = 0.6$ over the redshift range $0.0 < z < 3.0$, and for the 10 bins we use intervals of $\Delta z = 0.3$. The convergence power spectra for the 10 bins, together with the respective sample variance errors averaged over bands in l are shown in Fig. 1.

3.3 Fisher matrices for weak lensing

If the convergence field is Gaussian, and the noise is a combination of Gaussian-shape and instrument noise with no intrinsic correlations, the Fisher matrix is given by

$$F_{\alpha\beta} = \sum_{\ell=\ell_{\rm min}}^{\ell_{\rm max}} \frac{1}{(\Delta P_\kappa)^2} \frac{\partial P_\kappa}{\partial p^\alpha} \frac{\partial P_\kappa}{\partial p^\beta}, \tag{22}$$

where the uncertainty in the observed weak lensing spectrum is given by (Kaiser 1992, 1998)

$$\Delta P_\kappa(\ell) = \sqrt{\frac{2}{(2\ell+1) f_{\rm sky}}} \left[P_\kappa(\ell) + \frac{\langle {\gamma_{\rm int}}^2 \rangle}{\bar{n}} \right], \tag{23}$$

where $f_{\rm sky} = \Theta^2\pi/129\,600$ is the fraction of the sky covered by a survey of dimension Θ in degrees, and $\langle \gamma_{\rm int}^2 \rangle^{1/2}$ is the intrinsic ellipticity of galaxies. Guided by previous studies and taking into consideration the major difficulty of constraining both w_0 and w_1, we considered an almost full-sky ground-based-like survey with $f_{\rm sky} = 0.7$, a median redshift of roughly 1, an average galaxy number density of $\bar{n} = 30\,{\rm gal\,arcmin^{-2}}$, and $\langle \gamma_{\rm int}^2 \rangle^{1/2} = 0.4$. We also modelled an ambitious space-based-like survey with $f_{\rm sky} = 0.01$, 0.10, and 0.70, a median redshift of roughly 1.5, $\bar{n} = 100\,{\rm gal\,arcmin^{-2}}$, and $\langle \gamma_{\rm int}^2 \rangle^{1/2} \approx 0.25$. We have used $\ell_{\rm max} = 3000$ because, on smaller scales, the assumption of a Gaussian shear field underlying equation (20) and the HALOFIT approximation to the non-linear power spectrum may not be valid for larger values of ℓ. For the minimum ℓ, we take the fundamental mode approximation:

$$\ell_{\rm min} \approx \frac{360^\circ}{\Theta} = \sqrt{\frac{\pi}{f_{\rm sky}}}; \tag{24}$$

that is, we consider only lensing modes for which at least one wavelength can fit inside the survey area. For tomography, the Fisher matrix is generalized using

$$F_{\alpha\beta} = \sum_{\ell_{\rm min}}^{\ell_{\rm max}} (\ell + 1/2) f_{\rm sky} {\rm Tr} \left(\mathbf{C}_\ell^{-1} \frac{\partial \mathbf{P}_\ell}{\partial p^\alpha} \mathbf{C}_\ell^{-1} \frac{\partial \mathbf{P}_\ell}{\partial p^\beta} \right), \tag{25}$$

where $\mathbf{C}_\ell$ is the covariance matrix of the multipole moments of the observables $C_\ell^{\kappa\kappa'} = P_\ell^{\kappa\kappa'} + N_\ell^{\kappa\kappa'}$, with $N_\ell^{\kappa\kappa'} = \delta_{\kappa\kappa'} \langle \gamma_{\rm int}^2 \rangle / \Phi_i \bar{n}$ the power spectrum of the noise in the measurement. 'Tr' stands for 'trace'.

3.4 Weak lensing systematic effects

The probes considered here have systematic errors and nuisance factors that need to be well understood and well controlled in order for these constraints to be achievable. For cosmic shear, several systematic effects have been identified so far; see Refregier (2003) and references therein for an overview.

In this analysis, we included the effect of the shear calibration bias (Erben et al. 2001; Bacon et al. 2001; Hirata & Seljak 2003; Bernstein & Jarvis 2002; Kaiser 2000; Van Waerbeke & Mellier 2003) on our results by marginalizing over its parameters. In this bias, the shear is systematically over- or under-estimated by a multiplicative factor, and mimics an overall rescaling of the shear power spectrum. We used the absolute power calibration parameter $\zeta_{\rm s}$ and the relative calibration parameter $\zeta_{\rm r}$ between two redshift bins, following the parametrization used and discussed in Ishak et al. (2004). The calibration bias is not detected by the usual systematic tests such as the E- and B-mode decomposition of the shear field and the cross-correlation of the shear maps against the point spread function (PSF) maps. In a weak lensing survey, $\zeta_{\rm s}$ and $\zeta_{\rm r}$ are parameters of the experiment that can in principle be determined by detailed simulations of the observations. We impose in this analysis a reasonable Gaussian prior of 0.04 on these parameters.

Another serious systematic is the incomplete knowledge of the source redshift distribution (Wittman et al. 2000; Ishak & Hirata 2005), including the redshift bias and scattering. One can argue that, as long as the scatter in the redshift ($\sigma(z) \approx 0.05$) is much smaller than the width of the redshift bin $\Delta z = 0.3$ (for our 10-bin tomography), the effect on the integrated results should be small. This is because the scatter will only change slightly the shape of the edges of the window function that is used for the redshift integration within each bin. In contrast, the redshift bias alters the overall distribution and has been known to affect significantly the cosmological parameter estimation (Refregier 2003; Ishak et al. 2004; Tereno et al. 2005). A remedy to this poor knowledge of the redshift distribution using spectroscopic redshift has been explored recently in (Ishak & Hirata 2005). In the present analysis we marginalize over the redshift bias by including the characteristic redshift of the distribution as a systematic parameter $z_{\rm s}$, and we assume a reasonable Gaussian prior of 0.05 on this parameter.

It is important to question our assumption that the two weak lensing systematic errors that we considered here are Gaussian. All studies to date have made this assumption. The motivation for this assumption is the simplicity of the approximation, but its justification needs to be addressed in dedicated lensing systematic studies. Thus our treatment of these two systematics is only valid under this assumption of Gaussianity. For the redshift bias, one has to stress the requirement for a sufficiently large number of spectroscopic redshifts, see for example Ishak & Hirata (2005), and a sufficiently large number of source galaxies in order to reduce the uncertainties to a point where they can be approximated by Gaussians. Furthermore, more narrow-band colours and more accurate magnitudes (i.e. deeper exposure) are necessary in order to break degeneracies between the photometric redshifts. For the shear calibration bias, the errors cannot be made small enough by adding more data, and in this case simulations are necessary in order to estimate and address the question of non-Gaussianity. Massive sky image simulations on which the shear is measured and compared with the input will be necessary, and there are plans to carry out such studies within ongoing projects in the lensing community, for example the Shear TEsting Programme (STEP) project (see e.g. Heymans et al. 2005). Indeed, studying the shear calibration bias using massive simulations is one of the goals of this project (Heymans et al. 2005). Hence, the reader should be aware that our treatment of shear calibration errors is valid only under the Gaussianity assumption, and this needs to be checked by future simulation studies.

Finally, it is important to recall that there are systematic effects that were not included in this analysis [for example intrinsic alignments of galaxies, uncertainties associated with the non-linear mapping of the matter power spectrum; see Refregier (2003) and references therein for a list of other effect]. It is encouraging, however, to note that much effort has been put into studying these and other lensing systematic effects and that some progress has been made. With a better understanding of these limiting factors it will be possible to parametrize them and evaluate their effect on the cosmological parameter estimation.

4 PROBING DARK ENERGY WITH TYPE IA SUPERNOVAE

Type Ia supernovae are powerful probes of dark energy, as when properly calibrated they become cosmological standard candles that

can be used to measure distances as a function of redshift. The luminosity distance to a SN Ia is given by

$$d_{\rm L} \equiv \sqrt{\frac{L}{4\pi F}}, \tag{26}$$

where L is the intrinsic luminosity and F is the observed flux. The apparent magnitude of this SNa Ia can be written as

$$m = 5\ \log_{10}(D_{\rm L}) + \mathcal{M}, \tag{27}$$

where $D_{\rm L} \equiv H_0 d_{\rm L}/c$ is the dimensionless luminosity distance, $\mathcal{M} \equiv M - 5\log_{10}(H_0/c)$+constant is the magnitude parameter, and M is the absolute magnitude, degenerate here with the Hubble parameter. In a spatially flat model

$$D_{\rm L}(z) = (1+z)\ \int_0^z \frac{1}{\sqrt{(1-\Omega_\Lambda)(1+z')^3 + \Omega_\Lambda \mathcal{E}(z')}}\,{\rm d}z', \tag{28}$$

where $\mathcal{E}(z)$ is as defined in equation (2). We use the Fisher matrix for the SNe Ia defined as (see, for example, Tegmark et al. 1998; Huterer & Turner 2001)

$$F_{\alpha\beta} = \sum_{i=1}^{N} \frac{1}{\sigma_{\rm m}(D_{{\rm L},i})^2} \frac{\partial D_{{\rm L},i}}{\partial p^\alpha} \frac{\partial D_{{\rm L},i}}{\partial p^\beta}. \tag{29}$$

We use two sets of 2000 SNe Ia uniformly distributed with $z_{\rm max} = 0.8$ and $z_{\rm max} = 1.5$. It is important to note briefly that there are systematic uncertainties associated with supernova searches: these include luminosity evolution, gravitational lensing and dust; see, for example, Aldering et al. (2005) and references therein. In order partially to include the effect of these systematics and the effect of the supernova peculiar velocity uncertainty (Tonry et al. 2003), we follow Kim et al. (2004) and Upadhye et al. (2005) and use the following expression for the effective magnitude uncertainty:

$$\sigma_{\rm m}^{\rm eff} = \sqrt{\sigma_{\rm m}^2 + \left(\frac{5\sigma_{\rm v}}{\ln(10)cz}\right)^2 + N_{\{\rm per\ bin\}}\delta_{\rm m}^2}, \tag{30}$$

where a peculiar velocity of $\sigma_{\rm v} = 500\,{\rm km\,s^{-1}}$ is assumed, and, following Kim et al. (2004) and Upadhye et al. (2005), we use $\delta_{\rm m} = 0.02$ for space-based supernova survey data, and assume $\delta_{\rm m} = 0.04$ for ground-based survey data. The quadrature relation (28) ensures that there is an uncertainty floor set by the systematic limit $\delta_{\rm m}$ so that the overall uncertainty per bin cannot be reduced to arbitrarily low values by adding more supernovae.

5 PROBING DARK ENERGY WITH CMB AND COSMIC COMPLEMENTARITY

The CMB is a powerful cosmological probe; however, like other probes it suffers from some parameter degeneracies and needs to be combined with other data sets in order to provide tight constraints on dark energy parameters. For example, it is well known that cosmic shear and the CMB have different types of degeneracies in their parameters, which are nicely broken when these probes are combined. Indeed, among the orthogonal directions of degeneracy between cosmic shear and CMB are the known doublets ($\Omega_{\rm m}$, σ_8), (h, $n_{\rm s}$), and ($n_{\rm s}$, $\alpha_{\rm s}$) (see, for example, Tereno et al. 2005). We use this cosmic complementarity in the present analysis, where the statistical error (with some systematics included) on a given parameter p^α is given by

$$\sigma^2(p^\alpha) \approx \left[(\mathbf{F}_{\rm CMB} + \mathbf{F}_{\rm WL} + \mathbf{F}_{\rm SNe} + \Pi)^{-1}\right]^{\alpha\alpha}, \tag{31}$$

where Π is the prior curvature matrix, and $\mathbf{F}_{\rm CMB}$, $\mathbf{F}_{\rm WL}$ and $\mathbf{F}_{\rm SNe}$ are the Fisher matrices from the CMB, weak lensing, and supernovae, respectively. We impose only priors on the characteristic redshift and the calibration parameters by taking priors of $\sigma(z_{\rm p}) = 0.05$ and $\sigma(\zeta_{\rm s}) = \sigma(\zeta_{\rm r}) = 0.04$ on the calibration parameters [corresponding to 2 per cent rms uncertainty on the amplitude calibration; Hirata & Seljak (2003)]. We can add the CMB and weak lensing (WL) Fisher matrices together because the primary CMB anisotropies are generated at much larger comoving distances than the density fluctuations that give rise to weak lensing, and hence it is a good approximation to take them to be independent. For the CMB, we project constraints from 8 yr of *WMAP* data (WMAP8), 1 yr of *Planck* data (PLANCK1), and 1 yr of ACT data combined with WMAP8. The experiment specifications used for *Planck* and ACT are listed in Table 1. For the 8 yr of *WMAP* data, we include *TT*, *TE*, and *EE* power spectra, assuming $f_{\rm sky} = 0.768$ (the Kp0 mask of Bennet et al. 2003), temperature noises of 400, 480, and 580 μK arcmin in the *Q*, *V*, and *W*bands respectively (the rms noise was multiplied by $\sqrt{2}$ for polarization), and the beam transfer functions of Page et al. (2003).

6 RESULTS AND DISCUSSION

We calculated future constraints on dynamical dark energy parameters obtained from several combinations of cosmic microwave background (CMB) experiments, supernova (SNe Ia) searches, and weak lensing (WL) surveys with and without tomography. For the CMB, we considered future constraints from 8 yr of data from *WMAP* (WMAP8), one year of data from *Planck* (PLANCK1), and one year of data from the Atacama Cosmology Telescope (ACT1). We used two sets of 2000 supernovae, with $z_{\rm max} = 0.8$ (SN[0.8]) and $z_{\rm max} = 1.5$ (SN[1.5]) respectively, and considered various cosmic-shear reference surveys: an almost full sky (70 per cent) ground-based-like survey (WL) with successively two (WLT2) and five (WLT5) tomographic bins; and a deep-space-based-like survey with 10 tomographic bins (WLT10) covering successively 1, 10 and 70 per cent of the sky. We combined these experiments in doublets and triplets, taking into account space-based- or ground-based-like experiments for supernovae and weak lensing. The uncertainties

Table 1. CMB experiment specifications for *Planck* and ACT. The parameters used for WMAP8 are based on a projection of the one-year operation and are described in Section 5.

	$f_{\rm sky}$	$l_{\rm max}$	f(GHz)	θ_b(arcmin)	$(\Delta T/T)(10^{-6})$	$(\Delta P/T)(10^{-6})$
PLANCK1	0.8	2500	100	9.5	2.5	4.0
			143	7.1	2.2	4.2
			217	5.0	4.8	9.8
	$f_{\rm sky}$	$l_{\rm max}$	f(GHz)	θ_b(arcmin)	$w_{\rm eff}$ (sr^{-1})	
ACT1	0.005	8000	150	1.7	3×10^{18}	

Table 2. Summary of the parameter (w_0, w_1) estimation errors (1σ uncertainties) from various combinations of probes. CMB experiments are *WMAP* 8 yr, *Planck* 1 yr, and ACT 1 yr (unlensed spectra) combined with *WMAP* 8 yr. (We did not include constraints from the Sunayev–Zeldovich effect or lensing of the CMB, which ACT and *Planck* will help with.) The 2000 supernovae are uniformly distributed with $z_{\rm max} = 0.8$. WL is for a ground-based-like weak lensing survey with $f_{\rm sky} = 0.7, \bar{n} = 30\,{\rm gal\,arcmin^{-2}}$, $\langle\gamma_{\rm int}^2\rangle^{1/2} \approx 0.4$, and a median redshift $z_{\rm med} \approx 1$. WLT2 refers to the same weak lensing survey but with 2-bin tomography. The best constraints from the combinations in this Table are from PLANCK1+SN[0.8]+WLT2.

	CMB	+SN	+WL	+WLT2	+SN+WL	+SN+WLT2	SN+WL no-CMB	SN+WLT2 no-CMB
	WMAP8 alone							
$\sigma(w_0)$	3.73	0.25	0.66	0.35	0.21	0.11	0.24	0.11
$\sigma(w_1)$	5.65	0.87	1.45	0.66	0.59	0.26	0.93	0.35
	WMAP8+ACT							
$\sigma(w_0)$	0.82	0.20	0.58	0.22	0.18	0.11	”	”
$\sigma(w_1)$	1.87	0.59	1.40	0.42	0.48	0.25	”	”
	PLANCK1 alone							
$\sigma(w_0)$	0.50	0.17	0.28	0.23	0.093	0.086	”	”
$\sigma(w_1)$	0.31	0.23	0.20	0.18	0.083	0.069	”	”

Table 3. As Table 2, but for the dark energy parametrization (w_0, w_a). As usual, the errors on w_a are larger than those on w_1(roughly equal to twice the errors on w_1). The best constraints in this Table are from PLANCK1+SN[0.8]+WLT2.

	CMB	+SN	+WL	+WLT2	+SN+WL	+SN+WLT2	SN+WL no-CMB	SN+WLT2 no-CMB
	WMAP8 alone							
$\sigma(w_0)$	1.84	0.24	0.46	0.39	0.21	0.14	0.26	0.14
$\sigma(w_a)$	3.03	1.25	1.61	1.24	0.92	0.53	1.37	0.76
	ACT+WMAP8							
$\sigma(w_0)$	0.52	0.21	0.27	0.42	0.19	0.14	”	”
$\sigma(w_a)$	1.83	0.92	0.85	1.48	0.76	0.50	”	”
	PLANCK1 alone							
$\sigma(w_0)$	0.67	0.15	0.28	0.24	0.097	0.088	”	”
$\sigma(w_a)$	0.52	0.30	0.32	0.29	0.133	0.111	”	”

Table 4. Various tomography analyses: a comparative summary of the constraints (1σ uncertainties) on the various dark energy parametrizations from PLANCK1, 2000 uniformly distributed supernovae with $z_{\rm max} = 0.8$, 1.5, the ground-based-like lensing survey with successively 2- (WLT2) and 5-bin (WLT5) tomography, and the deep-space-based-like survey with 10-bin tomography (WLT10). The results are presented for the dark energy parameters $\{w_0, w_1\}$, $\{w_0, w_a\}$ and $\{\mathcal{E}_1 \equiv \rho_{\rm de}(z = 0.5)/\rho_{\rm de}(0), \mathcal{E}_2 \equiv \rho_{\rm de}(z = 1.0)/\rho_{\rm de}(0)\}$.

	PLANCK1 alone	+SN($z_{\rm max} = 1.5$)	+SN($z_{\rm max} = 0.8$) +WLT2[$f_{\rm sky} = 0.7$]	+SN(0.8)+WLT5 [$f_{\rm sky} = 0.7$]	+SN(1.5)+WLT10 [$f_{\rm sky} = 0.01$]	+SN(1.5)+WLT10 [$f_{\rm sky} = 0.1$]	+SN(1.5)+WLT10 [$f_{\rm sky} = 0.7$]
$\sigma(w_0)$	0.50	0.11	0.086	0.04	0.048	0.032	0.023
$\sigma(w_1)$	0.31	0.13	0.069	0.034	0.042	0.027	0.021
$\sigma(w_0)$	0.67	0.12	0.088	0.041	0.049	0.033	0.023
$\sigma(w_a)$	0.52	0.21	0.111	0.056	0.067	0.040	0.026
$\sigma(\mathcal{E}_1)$	0.11	0.048	0.029	0.012	0.013	0.010	0.009
$\sigma(\mathcal{E}_2)$	0.32	0.12	0.065	0.049	0.082	0.040	0.018

obtained on the dark energy parameters from CMB-only Fisher matrices should be treated with some caution as some of them are large and the Fisher matrix approximation may not be valid. We compared our CMB-only constraints for *Planck* with those of Hu (2001) and found them in good agreement. For example, when we fix the parameter w_1 to compare with Hu (2001), we find that our $\{\sigma(\Omega_\Lambda) = 0.087, \sigma(w) = 0.31\}$ are in good agreement with $\{\sigma(\Omega_\Lambda) = 0.098, \sigma(w) = 0.32\}$ from (Hu 2001). Importantly, the constraints we obtain from any combination of the three probes are significantly smaller than those from CMB-only, and therefore the constraints obtained are good estimates of the low bound of the uncertainties. Our results are summarized in Tables 2, 3, and 4 and in Figs 2, 3, 4, and 5. We looked for combinations of experiments that will provide constraints that are small enough

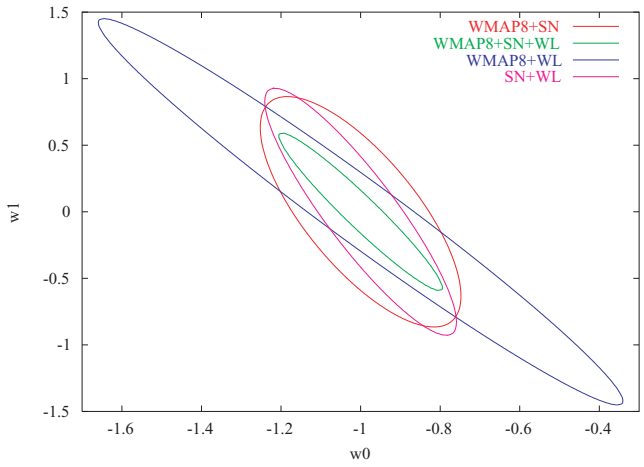

Figure 2. The 1σ confidence two-dimensional regions ($\Delta\chi^2 = 1$) for the (w_0, w_1) parameters. The plots contrast the constraints obtained from different combinations of 8 yr of data from *WMAP*, 2000 SNe Ia with $z_{\rm max} = 0.8$, and a ground-based-like WL reference survey with $f_{\rm sky} = 0.7$, $\bar{n} = 30\,{\rm gal\,arcmin}^{-2}$, $\langle\gamma_{\rm int}^2\rangle^{1/2} \approx 0.4$, and a median redshift $z_{\rm med} \approx 1$.

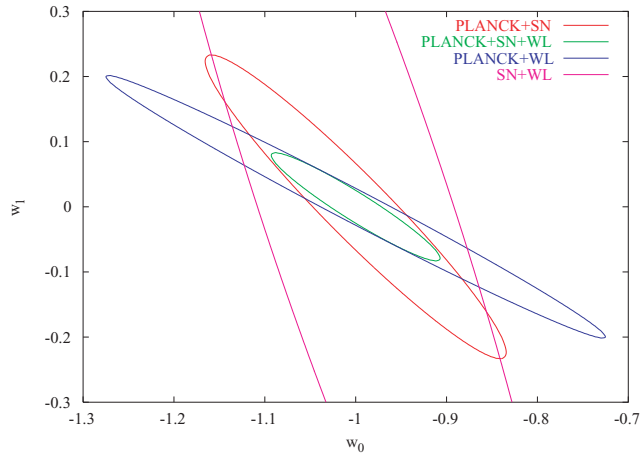

Figure 3. The 1σ confidence two-dimensional regions ($\Delta\chi^2 = 1$) for the (w_0, w_1) parameters. The plots contrast the constraints obtained from different combinations of 1 yr of data from *Planck*, 2000 SNe Ia with $z_{\rm max} = 0.8$, and a ground-based like WL reference survey with $f_{\rm sky} = 0.7$, $\bar{n} = 30\,{\rm gal\,arcmin}^{-2}$, $\langle\gamma_{\rm int}^2\rangle^{1/2} \approx 0.4$, and a median redshift $z_{\rm med} \approx 1$.

to answer conclusively some of the questions pertaining to dark energy.

The first question that merits an answer is whether dark energy is a cosmological constant or a dynamical component. The most decisive answer would be to rule out, using significant error bars, the cosmological constant. A less decisive but very suggestive answer would be to show that the dark energy parameters are those of a cosmological constant with an uncertainty of only a few per cent. This can be compared with the case of spatial curvature in the Universe: when CMB results constrained the total energy density to $\Omega_{\rm T} = 1.02 \pm 0.02$ at the 1σ level, it became generally more accepted that spatial curvature is negligible. However, it is important to note that it will always remain possible to build dark energy models that could have a set of parameters indistinguishable from those of a cosmological constant within the limits set. So, in this scenario, types of tests other than the equation of state will be required in order to close the question.

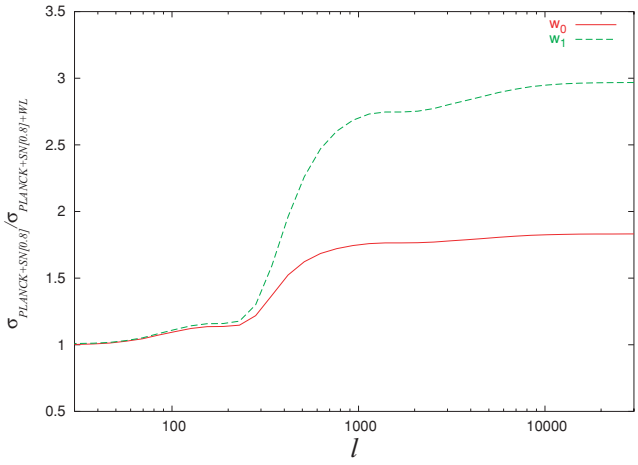

Figure 4. The improvement of the constraints as a function of the scales probed by the ground-based-like weak lensing survey (no tomography). The combination PLANCK1+SN[0.8]+WL is used here. The curves represent $\sigma_{\rm PLANCK1+SN[0.8]}/\sigma_{\rm PLANCK1+SN[0.8]+WL}$ for w_0 and w_1. The improvement from WL arises from probing non-linear scales ($l \gtrsim 100$), with a significant jump in the improvement between $l \sim 200$ and $\sim$2000 for the reference survey considered.

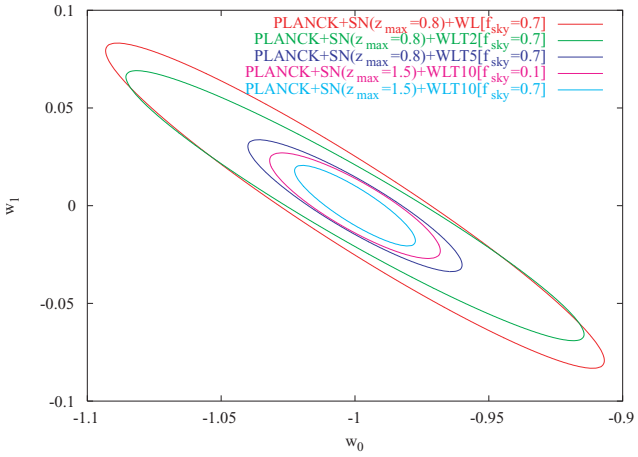

Figure 5. Tomography and the equation of state parameters: the 1σ confidence two-dimensional regions ($\Delta\chi^2 = 1$) for the parameters (w_0, w_1). The plots contrast the constraints from different combinations of 1 yr of data from *Planck*, 2000 uniformly distributed supernovae with $z_{\rm max} = 0.8, 1.5$, the ground-based-like lensing survey (WL), the ground-based-like survey with successively 2-bin tomography (WLT2) and 5-bin tomography (WLT5), and the deep-space-based-like survey with 10-bin tomography (WLT10).

As shown in Table 4, the combinations PLANCK1+SN[1.5]+WLT10[$f_{\rm sky} = 0.1$] and PLANCK1+SN[0.8]+WLT5[$f_{\rm sky} = 0.7$] provide impressive constraints that reach the goal set. This is followed in the table by the constraints from PLANCK1+SN[1.5]+WLT10[$f_{\rm sky} = 0.01$]. One should note here that, for the equation of state parameters, only small additional improvements to these constraints are obtained when an extremely ambitious sky coverage of 70 per cent is considered for PLANCK1+SN[1.5]+WLT10 [$f_{\rm sky} = 0.7$]. Finally, the constraints on the equation of state parameters from PLANCK1+SN[0.8]+WLT2[$f_{\rm sky} = 0.7$] are not small enough for the criterion of a few per cent set above.

Another test to answer the above question is to probe the dark energy density directly at various redshift points. For example, if future data show significant departures of the parameters $\mathcal{E}_1$ or $\mathcal{E}_2$

(see Section 2.2) from unity then a cosmological constant can be ruled out conclusively. Our analysis shows that this might be a less difficult test, as even PLANCK1+SN[0.8]+WLT5[$f_{\rm sky} = 0.7$] has the potential to achieve $\sigma(\mathcal{E}_1) = 0.012$ and $\sigma(\mathcal{E}_2) = 0.049$.

A second question of interest is what combination of experiments could distinguish between some of the currently proposed models of dark energy. Of particular interest are models that predict an equation of state with parameters that are significantly different from those of a cosmological constant. For example, one could consider quintessence tracker models (Zlatev, Wang & Steinhardt 1999) or super-gravity-inspired models (Brax & Martin 1999), for which, $w_0 \gtrsim -0.8$ and $\mathrm{d}w/\mathrm{d}z(z = 0) \sim 0.3$. From the Tables, we see that the distinction between these models and a cosmological constant can be achieved by several different combinations of experiments with different levels of precision.

Tables 2 and 3 show that, after combining PLANCK and supernova constraints, weak lensing without tomography adds an improvement of roughly a factor of 2 or better to the constraints. As shown in Fig. 4, the WL-improvement arises from probing non-linear scales ($l \gtrsim 100$), with a significant jump between $l \sim 200$ and $\sim$2000 for the ground-based-like survey considered. Adding 2-bin tomography to the lensing survey provides an additional factor of 2 improvement to the combination WMAP8+SN[0.8]+WL and to the combination ACT1+WMAP8+SN[0.8]+WL. We mention here that these results do not include constraints from the Sunayev–Zeldovich effect or lensing of the CMB, constraints that ACT and PLANCK will help with.

In Table 4 and Fig. 5 we summarize our results on multiple-bin tomography. The constraints on the equation of state parameters from PLANCK1+SN[1.5] improve by factors of 3–5 when WLT10 with $f_{\rm sky} = 0.1$ is added to the combination. Moeover, the constraints on the equation of state parameters from PLANCK1+SN[0.8]+WLT5[$f_{\rm sky} = 0.7$] are roughly factors of 3–6 better than those obtained from PLANCK1+SN[0.8]. Thus, we find that the improvements obtained from multiple-bin tomography lensing surveys are important for the questions raised at the beginning of this section, as they bring the uncertainties significantly closer to the goal of a few per cent. Therefore, the present study shows that tomography is very useful for adding further improvements to the constraints on dark energy parameters using both ground-based experiments and space-based experiments. The precise discussion of the technical and instrumental feasibility of multiple-bin tomography from the ground or from space is beyond the scope of this paper and should be addressed elsewhere.

We took care to include some systematic effects in our analysis. We parametrized the weak lensing calibration bias and assumed reasonable priors of 0.04 on the calibration parameters. We also parametrized the redshift bias and used a reasonable prior of 0.05. However, there are other systematic effects that we did not include and that may affect our results. For example, we did not include the effect of intrinsic correlations between the lensing source galaxies on our results (Croft & Metzler 2000; Heavens et al. 2000; Lee & Pen 2000; Catelan et al. 2001; Crittenden et al. 2001; Brown et al. 2002; Jing 2002; Jarvis et al. 2003; Heymans et al. 2004; Hirata & Seljak 2005), and we used the HALOFIT fitting formula to evaluate the non-linear matter power spectrum (full simulations should be used for real data analysis). As discussed in Section 3.4, our inclusion of these two lensing systematics assumed their Gaussianity. The effect of these systematics on our results is thus valid only under this approximation. Future dedicated studies of weak lensing systematic effects should address the issue of non-Gaussianity. In addition, following previous work, we included in our supernova constraints a conservative systematic limit, but more studies need to be done in this area as well.

Nevertheless, our results show that, after the combination of CMB, supernovae, and weak lensing surveys, tomography with very large fractions of the sky and many redshift bins has the potential to add key improvements to the dark energy parameter constraints by bringing them to the level of a few per cent.

On the other hand, the fact that very ambitious and sophisticated surveys are needed in order to achieve some of these constraints, and the difficulty in obtaining any further significant improvements, even with the most ambitious survey we considered, suggest the need for new tests to probe the nature of dark energy in addition to constraining its equation of state.

ACKNOWLEDGMENTS

The author thanks David Spergel for support and for useful discussions, and N. Bahcall, O. Doré, C. Hirata, P. Steinhardt, A. Upadhye, and L. Van Waerbeke for useful comments. The author acknowledges the support of the Natural Sciences and Engineering Research Council of Canada (NSERC) and the support of NASA Theory Award NNG04GK55G.

REFERENCES

Abazajian K., Dodelson S., 2003, Phys. Rev. Lett., 91, 041301
Aldering G. et al., 2005, PASP, submitted (astro-ph/0405232)
Bacon D. J., Refregier A., Clowe D., Ellis R.S., 2001, MNRAS, 325, 1065
Barris B. J. et al., 2004, ApJ, 602, 571
Benabed K., Van Waerbeke L., 2004, Phys. Rev. D, 70, 123515
Bennett C. L. et al., 2003, ApJS, 148, 1
Bernstein G. M., Jarvis M., 2002, AJ, 123, 583
Bernstein G. M., Jain B., 2004, ApJ, 600, 17
Blake C., Glazebrook K., 2003, AJ, 594, 665
Brax P., Martin J., 1999, Phys. Lett. B, 468, 40
Brown M.L., Taylor A. N., Hambly N.C., Dye S., 2002, MNRAS, 333, 501
Carroll S. M., Press W. H., Turner E. L., 1992, ARA&A, 30, 499
Catelan P., Kamionkowski M., Blandford R. D., 2001, MNRAS, 320, L7
Chevalier M., Polarski D., Starobinsky A., 2001, Int. J. Mod. Phys. D, 10, 213
Contaldi C. R., Hoekstra H., Lewis A., 2003, Phys. Rev. Lett., 90, 221303
Crittenden R. G., Natarajan P., Pen U.-L., Theuns T., 2001, ApJ, 559, 552
Crof R., Metzler C., 2000, ApJ, 545, 561
Eisenstein D. J., 2002, in Brown M.J.I., Dey A., eds, ASP Conf. Ser. Vol. 280, Next Generation Wide-Field Multi-object Spectroscopy. Astron. Soc. Pac., San Francisco, p. 35
Erben T. et al., 2001, A&A, 366, 717
Filippenko A. V., Riess A. G., 1998, Phys. Rept., 307, 31
Freedman W. L., 2004, in Wolff S., Lauer T., eds, Proc. NOAO Workshop, Observing Dark Energy. In press. (astro-ph/0411176)
Garnavich P. M. et al., 1998, ApJ, 509, 74
Garnavich P. M. et al., 2002, BAAS, 34, 1233
Heavens A., 2003, MNRAS, 343, 1327
Heavens A., Refregier A., Heymans C., 2000, MNRAS, 319, 649
Heymans C., Brown M., Heavens A., Meisenheimer K., Taylor A., Wolf C., 2004, MNRAS, 347, 895
Heymans C. et al., 2005, MNRAS, submitted (astro-ph/0506112)
Hirata C., Seljak U., 2003, MNRAS, 343, 459
Hirata C., Seljak U., 2004, Phys. Rev. D, 70, 063526
Hoekstra H., 2004, MNRAS, 347, 1337
Hu W., 1999, ApJ, 522, L21
Hu W., 2001, Phys. Rev. D, 65, 023003
Hu W., 2002, Phys. Rev. D, 66, 083515
Hu W., Tegmark M., 1999, ApJ, 514, L65
Huterer D., 2002, Phys. Rev. D, 65, 063001
Huterer D., Turner M. S., 2001, Phys. Rev. D, 64, 123527

Ishak M., 2005, preprint (astro-ph/0504416)
Ishak M., Hirata C., 2005, Phys. Rev. D, 71, 023002
Ishak M., Hirata C. M., McDonald P., Seljak U., 2004, Phys. Rev. D, 69, 083514
Jain B., Seljak U., 1997, ApJ, 484, 560
Jain B., Taylor A., 2003, Phys. Rev. Lett., 91, 141302
Jarvis M., Bernsetin G. M., Fischer P., Smith D., Jain B., Tyson J.A., Wittman D., 2003, AJ, 125, 1014
Jing Y. P., 2002, MNRAS, 335, L89
Kaiser N., 1992, ApJ, 388, 272
Kaiser N., 1998, ApJ, 498, 26
Kaiser N., 2000, ApJ, 537, 555
Kim A. G., Linder E. V., Miquel R., Mostek N., 2004, MNRAS, 347, 909
Kirshner R. P. et al., 2003. American Astronomical Society Meeting 202, #23.08 [see also http://www.ctio.noao.edu/wsne]
Knop R. A. et al., 2003, ApJ, 598, 102
Kosowsky A., 2003, New Astron. Rev., 47, 939
Lee J., Pen U., 2000, ApJ, 532, L5
Linder E., 2003a, Phys. Rev. Lett., 90, 091301
Linder E., 2003b, Phys. Rev. D., 68, 083504
Linder E., 2004, Phys. Rev. D., 70, 061302
Linder E., Jenkins A., 2003, MNRAS, 346, 573
Ma C.-P., Caldwell R. R., Bode P., Wang L., 1999, ApJ, 521, L1
Madgwick D. S., Hewett P. C., Mortlock D. J., Wang L., 2003, ApJ, 599, L33
Maor I., Brustein R., Steinhardt P. J., 2001, Phys. Rev. Lett., 86, 6 (Erratum, Phys. Rev. Lett., 87, 049901)
Maor I., Brustein R., McMahon J., Steinhardt P.J., 2002, Phys. Rev. D, 65, 123003
Mandelbaum R., McDonald P., Seljak U., Cen R., 2003, MNRAS, 344, 776
Massey R. et al., 2004, AJ, 127, 3089
Massey R., Refregier A., Bacon D.J., Ellis R., Brown M.L., 2005, MNRAS, 359, 1277
Mellier Y. et al., 2001, Mining the Sky. Springer-Verlag, Heidelberg
Mohr J. J., 2005, in Wolff S. C., Lauer T. R., eds, ASP Conf. Ser. Vol. 339, Observing Dark Energy. Astron. Soc. Pac., San Francisco, in press (astro-ph/0408484)
Padmanabhan T., 2003, Phys. Rep., 380, 335
Page L. et al., 2003, ApJS, 148, 37
Pain R., SNLS Collaboration, 2002, Bull. Am. Astron. Soc., 34, 1169
Perlmutter S. et al., 1997, Bull. Am. Astron. Soc., 29, 1351
Perlmutter S. et al., 1999, ApJ, 517, 565
Pritchet C. J., 2005, in Wolff S. C., Lauer T. R., eds, ASP Conf. Ser. Vol. 339, Observing Dark Energy. Astron. Soc. Pac., San Francisco, in press (astro-ph/0406242)
Refregier A., 2003, ARA&A, 41, 645
Refregier A. et al., 2004, AJ, 127, 3102
Riess A. G. et al., 1998, AJ, 116, 1009
Riess A. G. et al., 2000, ApJ, 536, 62
Riess A. G. et al., 2001, ApJ, 560, 49
Riess A. G. et al., 2004, ApJ, 607, 665
Rhodes J. et al., 2004, Astropart. Phys., 20, 377
Sahni V., Starobinsky A., 2000, Int. J. Mod. Phys. D, 9, 373
Seljak U. et al., 2005, Phys. Rev. D, 71, 103515
Seo H., Eisenstein D., 2003, AJ, 598, 720
Simon P., King L. J., Schneider P., 2004, A&A, 417, 873
Smith R. C. et al., 2002, Bull. Am. Astron. Soc., 34, 1232
Smith R. E. et al., 2003, MNRAS, 341, 1311
Song Y. S., Knox L., 2005, Phys. Rev. D, 70, 063510
Spergel L. et al., 2003, ApJS, 148, 175
Takada M., White M., 2004, ApJ, 601, L1
Takada M., Jain B., 2004, MNRAS, 348, 897
Tegmark M., Eisenstein D., Hu W., Kron R., 1998, astro-ph/9805117
Tereno I., 2005, ApJ, 429, 383
Tonry J. L. et al., 2003, ApJ, 594, 1
Turner M. S., 2000, Phys. Rep., 333, 619
Tyson J. A., 2002, in Tyson, J. A., ed., Proc. SPIE Vol. 4836, Survey and Other Telescope Technologies and Discoveries. Wolff, Sydney, p. 10
Upadhye A., Ishak M., Steinhardt P., 2005, Phys. Rev. D, 72, 063501
Van Waerbeke L. et al., 2002, A&A, 393, 369
Van Waerbeke L., Mellier Y., 2003, astro-ph/0305089
Wang Y., Freese K., 2004, astro-ph/0402208
Wang Y., Mukherjee P., 2004, ApJ, 606, 654
Wang Y., Tegmark M., 2004, Phys. Rev. Lett., 92, 241302
Wang X., Tegmark M., Jain B., Zaldarriaga M., 2003, Phys. Rev. D, 68, 123001
Weinberg S., 1989, Rev. Mod. Phys., 61, 1
Wittman D. M. 2002, in Tyson, J. A., ed., Proc. SPIE Vol. 4836, Survey and Other Telescope Technologies and Discoveries. Wolff, Sydney, p. 73
Wittman D. et al., 2000, Nat, 405, 143
Wood-Vasey W. M. et al., 2004, New Astron. Rev., 48, 637
Zlatev I., Wang L., Steinhardt P. J., 1999, Phys. Rev. Lett., 82, 896

This paper has been typeset from a TEX/LATEX file prepared by the author.